

Pisarenko's Formula for the Thermopower[†]

Andrei Novitskii,^a Takao Mori^{a,b,*}

The thermopower α (also known as the Seebeck coefficient) is one of the most fundamental material characteristics for understanding charge carrier transport in thermoelectric materials. Here, we revisit the Pisarenko formula for the thermopower, which was traditionally considered valid only for non-degenerate semiconductors. We demonstrate that regardless of the dominating scattering mechanism, the Pisarenko formula describes accurately enough the relationship between thermopower α and charge carrier concentration n beyond the non-degenerate limit. Moreover, the Pisarenko formula provides a simple thermopower-conductivity relation, $\alpha = \pm \frac{k_B}{e} (b - \ln \sigma)$, valid for materials with $\alpha > 90 \mu\text{V K}^{-1}$ when acoustic phonon scattering is predominant. This offers an alternative way to analyze electron transport when Hall measurements are difficult or inaccessible. Additionally, we show how the Pisarenko formula can be used to estimate the maximum power factor of a thermoelectric material from the weighted mobility of a single, not necessarily optimized, sample at any given temperature.

Thermoelectric materials are able to directly interconvert heat energy and electrical power, making them of particular interest for applications in solid-state cooling and power generation.^{1,2} Thermoelectric materials research typically aims to identify or develop materials with the best possible thermoelectric efficiency, defined by the figure of merit $zT = \alpha^2 \sigma T / (\kappa_{el} + \kappa_{lat})$, where α , σ , T and κ_{el} with κ_{lat} represent the thermopower, electrical conductivity, temperature, electronic and lattice (phonon) thermal conductivities, respectively. Improving zT is a non-trivial task due to the interrelationship among α , σ , κ_{lat} , and κ_{el} , mainly correlated through the charge carrier concentration n (chemical potential μ) and the scattering mechanisms involved.³ Therefore, understanding charge carrier transport properties is essential for engineering thermoelectric materials and enhancing their performance. Thermopower α , in turn, is a fundamental material parameter particularly helpful to understanding and optimizing thermoelectric materials. α depends on the band structure, charge carrier transport entropy, scattering mechanism, and the doping level of the material, leading its quantity to be a collection of many characteristics, including band degeneracy, effective mass, scattering factor, and chemical potential.⁴

The effective mass model is often used to analyze experimentally measured thermopower. For many semiconductors, charge carrier transport can be adequately described by considering the states near the band edge.⁵⁻⁷ When parabolic dispersion is assumed, the thermopower can be considered as the measure of the chemical potential μ (refer to the Supporting Information file for details).⁸ Experimental thermopower measurements, in turn, are relatively straightforward to perform and highly widespread, particularly in laboratories focused on thermoelectric materials research. A common approach is to fit the experimental data to the form expected for a semiconductor with a single parabolic band, where charge transport is dominated by a single scattering mechanism (e.g., acoustic phonon scattering), and the effective mass m_d^* independent of doping level and temperature. However, many materials deviate from this idealized scenario,⁹ exhibiting

multi-valley band structures,^{10,11} non-parabolic bands,¹² complex scattering mechanisms,¹³ or disorder that affects the carrier transport.^{14,15} Nevertheless, even in such cases lying beyond the single parabolic band approximation, the effective mass model remains one of the most simple yet useful tools for transport properties analysis, guiding rational design toward better thermoelectric performance.^{16,17}

Within the effective mass model, where carrier transport is dominated by majority carriers and described by a single parabolic band with a single scattering mechanism, the carrier relaxation time τ can be expressed by a simple power-law $\tau(\epsilon) = \tau_0 \epsilon^r$ with r representing the scattering factor. Consequently, the thermopower at any temperature or doping level can be described as a function of only chemical potential:^{5,7}

$$\alpha(\eta) = \pm \frac{k_B}{e} \left(\frac{(r+5/2) F_{r+3/2}(\eta)}{(r+3/2) F_{r+1/2}(\eta)} - \eta \right), \quad (1)$$

where k_B is the Boltzmann constant, e is the electron charge, and $F_j(\eta)$ is the j -th order Fermi integrals defined as

$$F_j(\eta) = \int_0^\infty \frac{\epsilon^j}{1 + e^{\epsilon - \eta}} d\epsilon, \quad (2)$$

with $\epsilon = E/k_B T$ representing the reduced carrier energy, and $\eta = \mu/k_B T$ representing the reduced chemical potential. The charge carrier concentration in this context is given by

$$n(\eta) = 4\pi \left(\frac{2m_d^* k_B T}{h^2} \right)^{3/2} F_{1/2}(\eta), \quad (3)$$

where m_d^* is the density-of-state effective mass, h is the Planck constant. Therefore, the effective mass m_d^* value can be estimated from experimental values of thermopower α and carrier concentration n . For practical purposes, however, it is convenient to use analytical expressions that directly connect α and n , avoiding numerical integration of the Fermi integrals (Eq. 2). For the two limiting cases of a degenerate ($\eta \geq 5$) and a non-degenerate ($\eta \leq -1$) semiconductors, the Fermi integrals can be solved analytically, providing relatively simple expressions for the transport coefficients (for details, refer to Supporting Information; Figure S1). Note that the band edge ($\eta = 0$) is used as the reference point for the chemical potential.^{5,6}

^aResearch Center for Materials Nanoarchitectonics (MANA), National Institute for Materials Science (NIMS), 1-1 Namiki, Tsukuba, Ibaraki, 305-0044, Japan.

^bGraduate School of Pure and Applied Sciences, University of Tsukuba, 1-1-1 Tennodai, Tsukuba, Ibaraki, 305-8573, Japan.

*E-mail: MORI.Takao@nims.go.jp.

[†]Electronic supplementary information available.

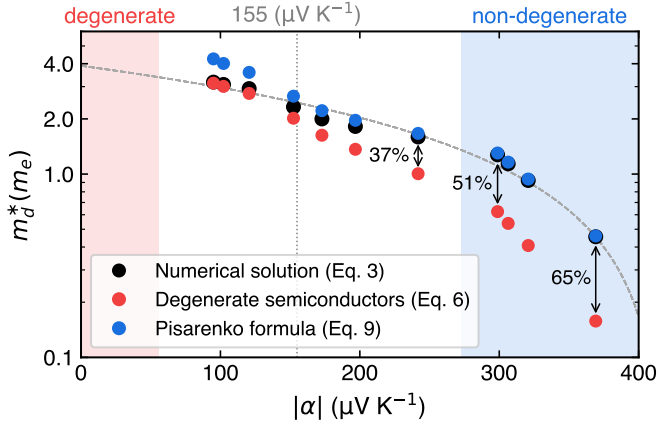


Figure 1 Effective mass m_d^* as a function of the thermopower α , calculated from the experimental data of $\text{Yb}_x\text{Co}_4\text{Sb}_{12}$ (Ref. 19) using the numerical solution (Eq. 3, black symbols), and two analytical formulas, namely, for degenerate semiconductors (Eq. 6, red symbols) and Pisarenko formula (Eq. 9, blue symbols). Acoustic phonon scattering was assumed ($r = -1/2$). The vertical gray dotted line indicates the threshold α value ($\approx 155 \mu\text{V K}^{-1}$), below which Eq. 6 provides more accurate m_d^* estimates. The black arrows indicate underestimation of m_d^* when Eq. 6 is used for $\alpha > 155 \mu\text{V K}^{-1}$. The gray dashed curve is a guide to the eye to visualize the general trend.

In the degenerate limit, Fermi integrals (Eq. 2) can be expressed as a power series through the Sommerfeld expansion, thereby reducing Eqs. 1 and 3 to

$$\alpha(\eta) = \pm \frac{k_B}{e} \frac{\pi^2}{3} \frac{r+3/2}{\eta} \quad (\eta \geq 5) \quad (4)$$

and

$$n(\eta) = \frac{8\pi}{3} \left(\frac{2m_d^* k_B T}{h^2} \right)^{3/2} \eta^{3/2} \quad (\eta \geq 5). \quad (5)$$

By combining Eqs. 4 and 5, one obtains the well-known formula for the thermopower in degenerate semiconductors:⁷

$$\alpha = \pm \frac{8\pi^2 k_B^2 T}{3eh^2} m_d^* \left(\frac{\pi}{3n} \right)^{2/3} \left(r + \frac{3}{2} \right). \quad (6)$$

While some thermoelectric materials can indeed be considered degenerate semiconductors, most are actually only partially degenerate ($-1 < \eta < 5$). Partially degenerate semiconductors can exhibit features of both degenerate and non-degenerate semiconductors (e.g., metallic-like behavior of $\sigma(T)$ along with high α values), often observed in thermoelectric materials.³ Moreover, properly optimized materials usually have a chemical potential η close to the band edge ($\eta_{opt} \approx 0$, $\alpha_{opt} \approx 200 \mu\text{V K}^{-1}$),^{16,18} which can result in significant underestimation of the effective mass by up to 30% when using Eq. 6 (Figures 1, S2).

In the non-degenerate region, Fermi-Dirac statistics can be replaced by Boltzmann statistics, simplifying Eq. 1 for the thermopower to

$$\alpha(\eta) = \pm \frac{k_B}{e} \left(r + \frac{5}{2} - \eta \right) \quad (\eta \leq -1). \quad (7)$$

Similarly, the carrier concentration in the bandgap is expressed as

$$n(\eta) = 2 \left(\frac{2\pi m_d^* k_B T}{h^2} \right)^{3/2} e^\eta \quad (\eta \leq -1). \quad (8)$$

Accordingly, using both Eqs. 7 and 8, the relation between α and n for non-degenerate semiconductors could be expressed as:

$$\alpha = \pm \frac{k_B}{e} \left(r + \frac{5}{2} + \ln \left[\frac{2(2\pi m_d^* k_B T)^{3/2}}{h^3 n} \right] \right). \quad (9)$$

This relation, commonly referred to as the Pisarenko formula, is believed to have been derived by Nikolai Pisarenko between 1936 and 1940. However, the historical attribution of the Pisarenko formula (Eq. 9) remains unclear. While it is indeed widely associated with Pisarenko, there is no evidence that he ever published this formula.²⁰ The first explicit mention of Pisarenko's contributions to thermoelectricity appears in the 1940 review paper by Davydov and Shmushkevich, where they noted that most of the formulas describing galvanomagnetic, thermomagnetic, and thermoelectric effects (including Eq. 9) in non-degenerate semiconductors were derived by Pisarenko.²¹ However, Matvei Bronstein

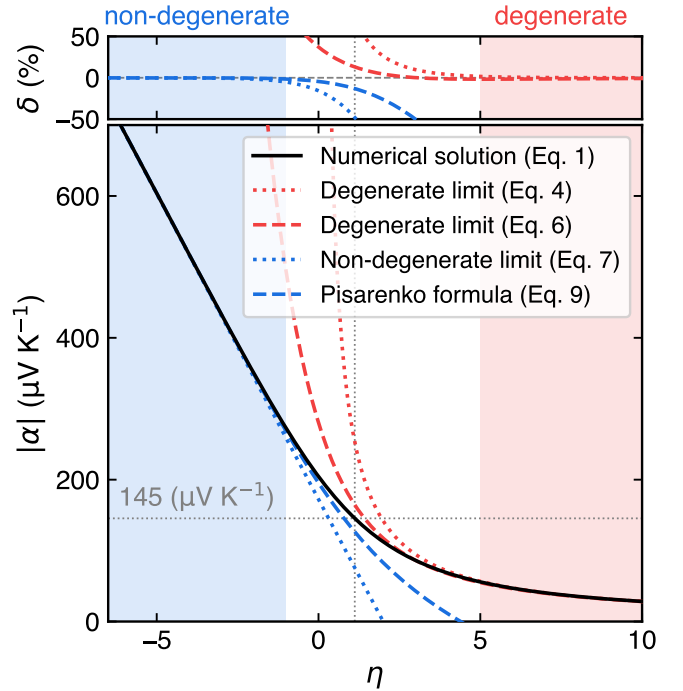


Figure 2 Thermopower α as a function of the chemical potential η , calculated using the numerical solution (Eq. 1, black solid curve), the degenerate limit (Eq. 4, red dotted curve), the non-degenerate limit (Eq. 7, blue dotted curve), and two analytical formulas for degenerate (Eq. 6, red dashed curve) and non-degenerate (Pisarenko formula, Eq. 9, blue dashed curve) semiconductors within the acoustic phonon scattering approximation ($r = -1/2$). The upper panel shows δ , the relative difference in α calculated using the corresponding formulas. The thin gray dotted lines indicate the threshold where δ between α values calculated from Eq. 6 and Eq. 9 is equal and reaches $\approx 13\%$, representing the limits of their applicability.

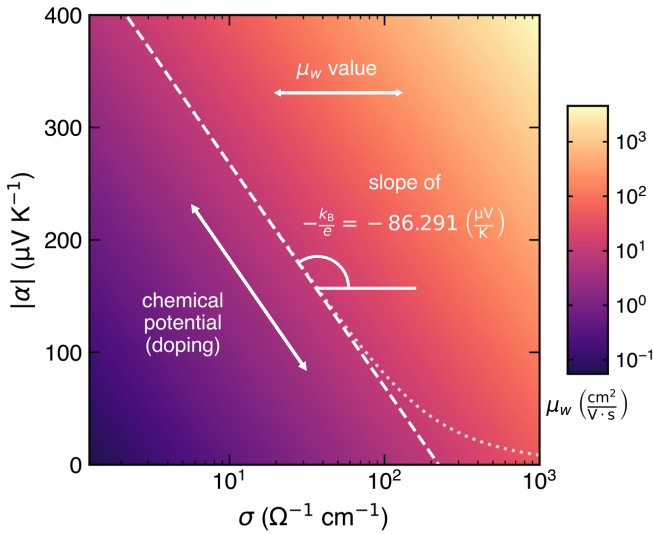


Figure 3 A Jonker plot (α vs. log-scale σ), schematically displaying the thermopower-conductivity relation as predicted by the Pisarenko formula (Eq. 11, white dashed line) and the full numerical solution (Eq. 1, light gray dotted curve). The slope of the Pisarenko line is $\pm k_B/e \approx \pm 86.291 \mu\text{V K}^{-1}$ (positive slope for n -type semiconductors and a negative slope for p -type semiconductors), while its horizontal position is determined by the weighted mobility μ_w value.

apparently first studied these effects in non-degenerate semiconductors in 1932 – 1933.^{22,23} In his papers, Bronstein provided the classical relation for $\alpha(\eta)$ in the non-degenerate limit (Eq. 7), as well as a precursor to the Pisarenko formula connecting α and n . Given the overlapping timeline, it is possible that Pisarenko and Bronstein collaborated or worked in parallel, but the historical records remain ambiguous. It is worth noting that Bronstein's contributions to semiconductor physics were cut short by his execution in 1938 during the Great Purge, and citing his works during that period may have been considered dangerous.²⁴ Even so, Davydov and Shmushkevich included references to Bronstein's research in their 1940 paper, indicating its foundational importance. The question of Pisarenko's specific role in deriving the relation that now bears his name thus remains an open topic for historical investigation.²⁵

At first glance, the limits of applicability of the Pisarenko formula (Eq. 9) should match those of the classical Bronstein formula (Eq. 7). However, as initially noted by Yu.P. Maslakovets and later confirmed by T.A. Kontorova,²⁶ this is not the case. The Pisarenko formula (Eq. 9), in fact, agrees with the numerical solution (Eq. 1) beyond non-degenerate limit up to $\eta \approx 1$ with an error of less than 10% (Figure 2). Therefore, the Pisarenko formula accurately describes $\alpha(n)$ relationship for materials with $|\alpha| > 150 \mu\text{V K}^{-1}$ (Figure S3). For higher degrees of degeneracy ($\eta > 1$ and $|\alpha| < 150 \mu\text{V K}^{-1}$), Eq. 6 for degenerate semiconductors provides a better accuracy (Figures 2, S3). This result is independent of temperature or the value of the effective mass. The only parameter affecting the agreement between the analytical formulas and the full numerical solution in the intermediate degeneracy region is the scattering factor r . It is important to note that in the main text, we present and discuss results under

the assumption of acoustic phonon scattering ($r = -1/2$). Acoustic phonon scattering is indeed one of the most common scattering mechanisms, frequently observed in semiconducting materials at or above room temperature. However, in some materials, particularly those promising for thermoelectric applications, charge carrier scattering is reported to be dominated by polar optical ($r = 1/2$) or ionized impurity ($r = 3/2$) scattering, respectively.^{27–31} As such, we provide results for $r = 1/2$ and $3/2$ in the Supporting Information and demonstrate that the Pisarenko formula remains valid for α values higher than $130 - 150 \mu\text{V K}^{-1}$ regardless of the scattering mechanism (Figures S4, S5).

However, analyzing the thermopower α as a function of carrier concentration n is limited since it still requires data from Hall measurements. For materials with high electrical resistivity and/or low charge carrier mobility, Hall measurements can be difficult or even impossible to perform. Additionally, the interpretation of the Hall data can be complicated for materials with a pronounced contribution from the anomalous Hall effect. From a practical perspective, it is much more convenient to analyze the relationship between α and σ , both of which can be readily measured over a wide temperature range, whereas Hall measurements are typically performed at or below room temperature. Similar to how $\alpha(n)$ relations are derived (Eqs. 6 and 9), $\alpha(\sigma)$ relations can also be obtained for both degenerate and non-degenerate regions (see Supporting Information for details):

$$\alpha = \pm \frac{k_B}{e} \frac{\pi^2}{3} \left(r + \frac{3}{2} \right) \left(\frac{\sigma_{E_0}}{\sigma} \right)^{\frac{1}{r+3/2}} \quad (10)$$

and

$$\alpha = \pm \frac{k_B}{e} \left(r + \frac{5}{2} + \ln \left[\Gamma \left(r + \frac{5}{2} \right) \frac{\sigma_{E_0}}{\sigma} \right] \right), \quad (11)$$

respectively. Here, Γ is the gamma function, and σ_{E_0} is the transport coefficient, which is merely a function of the weighted mobility μ_w :

$$\sigma_{E_0} = \frac{8\pi e (2m_e k_B T)^{3/2}}{3h^3} \mu_w. \quad (12)$$

The weighted mobility is given by $\mu_w = \mu_0 (m_d^*/m_e)^{3/2}$, where μ_0 represents the intrinsic carrier mobility, and m_e is the electron mass. Essentially, weighted mobility can be thought of as a descriptor of a material's inherent electronic transport properties, determining the maximum achievable power factor at a given temperature, as will be shown later. Furthermore, the weighted mobility can be considered an experimental parameter that, unlike the effective mass, can be easily calculated from the measured thermopower and electrical conductivity.³²

Eq. 11 provides a simple form of the thermopower-conductivity relationship:

$$\alpha = \pm \frac{k_B}{e} (b - \ln \sigma) \quad (13)$$

with

$$b = r + \frac{5}{2} + \ln \left[\Gamma \left(r + \frac{5}{2} \right) \sigma_{E_0} \right] \quad (14)$$

and can be represented as a straight line with a slope of $\pm k_B/e \approx \pm 86.291 \mu\text{V K}^{-1}$ (positive slope for n -type semiconductors and a

negative slope for p -type semiconductors) on a linear α vs. $\log \sigma$ scale (Jonker plot, Figure 3). In the case of acoustic phonon scattering, the $\alpha(\sigma)$ relationship provided by the Pisarenko formula (Eq. 11) agrees with the numerical solution (Eq. 1) down to $\alpha \approx 90 \mu\text{V K}^{-1}$ (Figures 3, S6, S7). The prediction given by the Pisarenko formula (Eq. 11) is well substantiated by experiments, even though the materials under study were not necessarily single band or non-degenerate semiconductors (see Figure S8, for example).^{33–36} For many thermoelectric materials, the simultaneous change of α with σ upon rigid-band-like doping is indeed follows a slow logarithmic decrease.^{37–43} Moreover, as noted earlier, there exists a significant group of partially degenerate semiconductors in which the charge carrier concentration n , as well as the effective mass m_d^* , remain constant or change only slightly with temperature. For such materials, the Pisarenko formula (Eq. 9 or 11) sufficiently describes not only the $\alpha(n)$ (or $\alpha(\sigma)$) dependence, but also the temperature dependence of the thermopower (Figure S9). A well-known example of such partially degenerate semiconductors is p -type BiCuSeO oxyselenides, which exhibit thermopower values in the range of $300 - 400 \mu\text{V K}^{-1}$ across the entire temperature range. Upon aliovalent substitution of Bi (the most common approach to optimize n), however, the electrical conductivity switches to metal-like behavior (i.e., decreases with temperature), while the relatively high Seebeck coefficient remains preserved.⁴⁴ Therefore, the change in α and $\alpha^2\sigma$ with σ upon doping quite closely follows the Pisarenko formula, as shown in Figure 4. The experimental data align well with the predicted curves, corresponding to μ_w values between 10 and $22.5 \text{ cm}^2 \text{ V}^{-1} \text{ s}^{-1}$, respectively. This range of weighted mobility is likely due to varying degrees of grain boundary scattering of charge carriers caused by differences in processing conditions.⁴⁵ Interestingly, Figure 4 also highlights different strategies for achieving maximum power factor. For instance, in the work of Sui et al., the authors achieved the highest power factor by substituting Bi with Ba, yet limited due to low weighted mobility (black empty diamonds in Figure 4).⁴⁶ By using subsequent texturization, authors were able to enhance the weighted mobility nearly fivefold and, consequently, the power factor while maintaining the same charge carrier concentration since the stoichiometry of the samples remained unchanged. In this context, the Jonker plot analysis can serve as a complement to or an alternative to Hall measurements when they are not accessible. Even in cases beyond the single parabolic band approximation, analyzing the thermopower-conductivity relationship can provide additional insights into electron transport in the material, such as the scattering mechanism,⁴⁷ changes in band structure,⁴⁸ etc.

Additionally, the applicability range of the Pisarenko formula (Eq. 11) should be sufficient to accurately describe the power factor $\alpha^2\sigma$ and predict its maximum, expected at $\eta \approx 0.67$ within the effective mass model. Considering Eq. 13, the power factor can be expressed as

$$\alpha^2\sigma = \left(\frac{k_B}{e}\right)^2 \sigma (b^2 - 2b \ln \sigma + (\ln \sigma)^2). \quad (15)$$

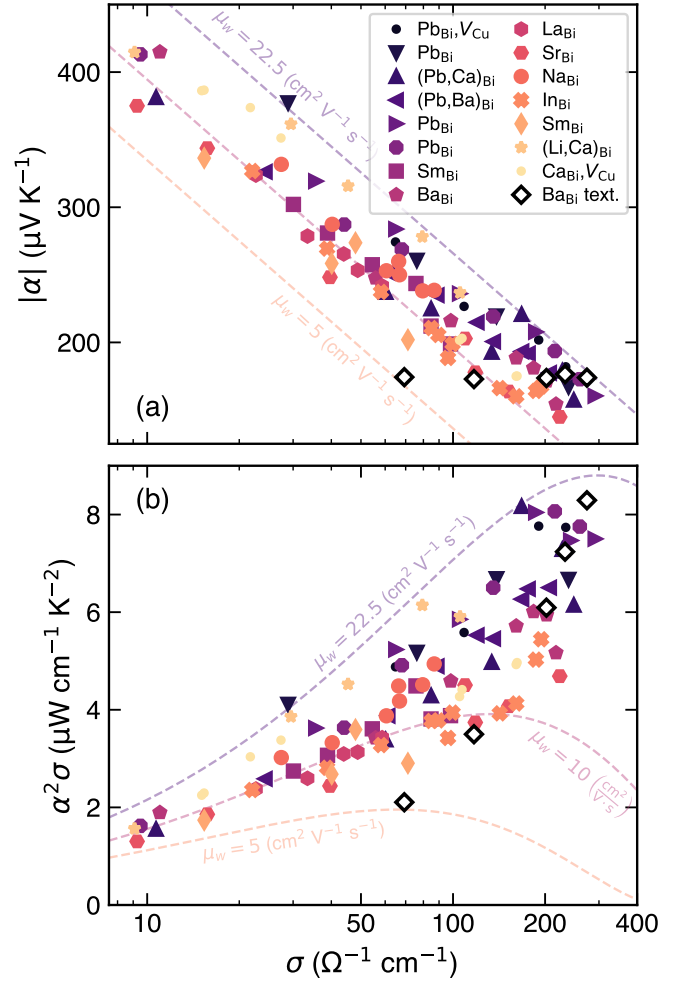


Figure 4 Experimental (a) thermopower α and (b) power factor $\alpha^2\sigma$ as a functions of electrical conductivity σ for doped BiCuSeO oxyselenides at 800 K (Refs. 43,46,49–62). Dashed lines represent the Pisarenko formula (Eq. 11) and the power factor-conductivity relation (Eq. 15), calculated for different values of weighted mobility μ_w . A portion of the literature data was retrieved from the StarryData2 database.⁶³

This expression, derived from the Pisarenko formula, agrees well with the full numerical solution and underestimates the maximum value of the power factor by only about 1.5% (Figure 5). The maximum power factor, in turn, can be determined from the condition $\frac{\partial(\alpha^2\sigma)}{\partial\sigma} = 0$, which yields $\ln \sigma = b - 2$. Therefore, in this simplified theoretical model, $(\alpha^2\sigma)_{\text{max}}$ depends only on r and μ_w (or σ_{E_0}):

$$(\alpha^2\sigma)_{\text{max}} = 4 \left(\frac{k_B}{e}\right)^2 e^{r+1/2} \Gamma\left(r + \frac{5}{2}\right) \sigma_{E_0}. \quad (16)$$

For acoustic phonon scattering ($r = -1/2$), Eq. 16 can be rewritten as

$$(\alpha^2\sigma)_{\text{max}} = 4 \left(\frac{k_B}{e}\right)^2 \frac{8\pi e (2m_e k_B T)^{3/2}}{3h^3} \mu_w \quad (17)$$

or

$$(\alpha^2\sigma)_{\text{max}} = 1.73 \cdot 10^{-5} T^{3/2} \mu_w, \quad (18)$$

where $(\alpha^2\sigma)_{\text{max}}$ is in $\mu\text{W cm}^{-1} \text{ K}^{-2}$ and μ_w in $\text{cm}^2 \text{ V}^{-1} \text{ s}^{-1}$. Hence,

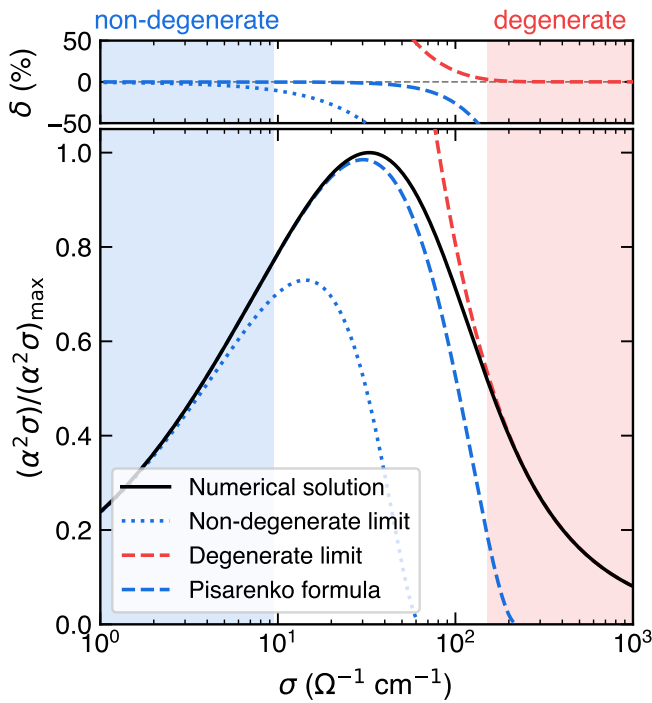


Figure 5 Normalized power factor $(\alpha^2\sigma)/(\alpha^2\sigma)_{\max}$ as a function of electrical conductivity σ calculated using the full numerical solution (black solid curve), the non-degenerate limit (blue dotted curve), the degenerate limit (red solid curve), and the Pisarenko formula (Eq. 15, blue solid curve) within the acoustic phonon scattering approximation ($r = -1/2$). The upper panel shows δ , the relative difference in $(\alpha^2\sigma)/(\alpha^2\sigma)_{\max}$ calculated using the corresponding formulas.

given only the electrical conductivity and thermopower of a single sample at an arbitrary doping level, Eq. 18 can provide a reasonable estimate of its highest power factor expected after optimizing its carrier concentration.

In conclusion, the Pisarenko formula (Eq. 9) offers a more accurate estimate of the effective mass than the formula for degenerate semiconductors (Eq. 6) when $|\alpha| > 150 \mu\text{VK}^{-1}$. The thermopower-conductivity relationship provided by the Pisarenko formula (Eq. 11) is valid for $|\alpha| > 90 \mu\text{VK}^{-1}$ ($r = -1/2$) and can be utilized to analyze electron transport in addition to or as an alternative to Hall measurements when those are not accessible. Furthermore, the Pisarenko formula can be readily used to estimate the maximum power factor achievable at a given temperature and weighted mobility.

Acknowledgements

This work was supported by JST Mirai JPMJMI19A1. The authors are grateful to Prof. Alexander Burkov (Ioffe Institute) and Prof. Jean-François Halet (University of Rennes) for fruitful discussions. A.N. also thanks Jenny Murakoshi, current and former Thermal Energy Materials Group (NIMS) members for plentiful discussions.

CRediT Statement

Andrei Novitskii: Conceptualization, Methodology, Investigation, Data Curation, Writing (Original Draft), Writing (Review & Editing), Visualization. **Takao Mori:** Writing (Review & Editing), Supervision, Funding Acquisition.

Conflicts of Interest

There are no conflicts to declare.

Data Availability Statement

Data sharing is not applicable to this article as no new data were created in this study.

Keywords

Pisarenko, Thermopower, Seebeck Coefficient, Effective Mass Model, Thermoelectrics

References

- 1 J. Mao, G. Chen and Z. Ren, *Nat. Mater.*, 2021, **20**, 454–461.
- 2 T. Hendricks, T. Caillat and T. Mori, *Energies*, 2022, **15**, 7307.
- 3 A. F. Ioffe, *Semiconductor Thermoelements, and Thermoelectric Cooling*, Infosearch, London, 1957.
- 4 L. Wang, X. Zhang and L.-D. Zhao, *Acc. Mater. Res.*, 2023, **4**, 448–456.
- 5 V. I. Fistul', *Heavily Doped Semiconductors*, Springer, New York, 1969.
- 6 P. S. Kireev, *Semiconductor Physics*, Mir Publishers, Moscow, 1978.
- 7 B. M. Askerov, *Electron Transport Phenomena in Semiconductors*, World Scientific, Singapore, 1994.
- 8 T. Takeuchi, Y. Toyama and A. Yamamoto, *Mater. Trans.*, 2010, **51**, 421–427.
- 9 J. de Boer, *J. Materiomics*, 2021, **7**, 603–611.
- 10 D. J. Singh and I. I. Mazin, *Phys. Rev. B*, 1997, **56**, R1650–R1653.
- 11 A. F. May, D. J. Singh and G. J. Snyder, *Phys. Rev. B*, 2009, **79**, 153101.
- 12 D. J. Singh and W. E. Pickett, *Phys. Rev. B*, 1994, **50**, 11235–11238.
- 13 Y. I. Ravich, B. A. Efimova and I. A. Smirnov, *Semiconducting Lead Chalcogenides*, Plenum, New York, 1970.
- 14 I. P. Zvyagin, *Kinetic Phenomena in Disordered Semiconductors* (in Russian), Moscow State University Press, Moscow, 1984.
- 15 V. F. Gantmakher, *Electrons and Disorder in Solids*, Oxford University Press, New York, 2005.
- 16 X. Zhang, Z. Bu, X. Shi, Z. Chen, S. Lin, B. Shan, M. Wood, A. H. Snyder, L. Chen, G. J. Snyder and Y. Pei, *Sci. Adv.*, 2020, **6**, eabc0726.
- 17 H. Wang, R. Gurunathan, C. Fu, R. Cui, T. Zhu and G. J. Snyder, *Mater. Adv.*, 2022, **3**, 734–755.
- 18 S. Kang and G. J. Snyder, 2017, <https://arxiv.org/abs/1710.06896>.
- 19 Y. Tang, Z. M. Gibbs, L. A. Agapito, G. Li, H.-S. Kim, M. B.

- Nardelli, S. Curtarolo and G. J. Snyder, *Nat. Mater.*, 2015, **14**, 1223–1228.
- 20 *200 Years of Thermoelectricity: An Historical Journey Through the Science and Technology of Thermoelectric Materials (1821–2021)*, ed. L. Anatyshuk, A. Burkov, J. Goldsmid, Y. Grin, K. Koumoto, D. Narducci and G. S. Nolas, Springer, Cham, 2024.
- 21 B. J. Davydov and I. M. Shmushkevich, *Usp. Fiz. Nauk*, 1940, **24**, 21–67.
- 22 M. Bronstein, *Phys. Z. Sowjetunion*, 1932, **2**, 28–45.
- 23 M. Bronstein, *Phys. Z. Sowjetunion*, 1932, **3**, 140–145.
- 24 G. E. Gorelik and V. Y. Frenkel, *Matvei Petrovich Bronstein and Soviet Theoretical Physics in the Thirties*, Birkhäuser Basel, 1994.
- 25 A. T. Burkov, personal communication.
- 26 T. A. Kontorova, *Zh. Tekh. Fiz.*, 1954, **24**, 1291–1297.
- 27 H. Wang, X. Cao, Y. Takagiwa and G. J. Snyder, *Mater. Horiz.*, 2015, **2**, 323–329.
- 28 J. Shuai, J. Mao, S. Song, Q. Zhu, J. Sun, Y. Wang, R. He, J. Zhou, G. Chen, D. J. Singh *et al.*, *Energy Environ. Sci.*, 2017, **10**, 799–807.
- 29 X. Shi, C. Sun, Z. Bu, X. Zhang, Y. Wu, S. Lin, W. Li, A. Faghaninia, A. Jain and Y. Pei, *Adv. Sci.*, 2019, **6**, 1802286.
- 30 Q. Ren, C. Fu, Q. Qiu, S. Dai, Z. Liu, T. Masuda, S. Asai, M. Hagihala, S. Lee, S. Torri *et al.*, *Nat. Commun.*, 2020, **11**, 3142.
- 31 A. M. Ganose, J. Park and A. Jain, 2022, <https://arxiv.org/abs/2210.01746>.
- 32 G. J. Snyder, A. H. Snyder, M. Wood, R. Gurunathan, B. H. Snyder and C. Niu, *Adv. Mater.*, 2020, **32**, 2001537.
- 33 G. Jonker, *Philips Res. Rep.*, 1968, **23**, 131–138.
- 34 M.-Y. Su, C. E. Elsbernd and T. O. Mason, *J. Am. Ceram. Soc.*, 1990, **73**, 415–419.
- 35 D. Rowe and G. Min, *J. Mater. Sci. Lett.*, 1995, **14**, 617–619.
- 36 S. D. Kang and G. J. Snyder, *Nat. Mater.*, 2017, **16**, 252–257.
- 37 M. Ohtaki, T. Tsubota, K. Eguchi and H. Arai, *J. Appl. Phys.*, 1996, **79**, 1816–1818.
- 38 E. S. Toberer, M. Christensen, B. B. Iversen and G. J. Snyder, *Phys. Rev. B*, 2008, **77**, 075203.
- 39 E. S. Toberer, A. F. May, B. C. Melot, E. Flage-Larsen and G. J. Snyder, *Dalton Trans.*, 2010, **39**, 1046–1054.
- 40 Q. Zhu, E. M. Hopper, B. J. Ingram and T. O. Mason, *J. Am. Ceram. Soc.*, 2011, **94**, 187–193.
- 41 F. Ahmed, N. Tsujii and T. Mori, *J. Mater. Chem. A*, 2017, **5**, 7545–7554.
- 42 G. Guélou, F. Failamani, P. Sauerschnig, J. Waybright, K. Suzuta and T. Mori, *J. Mater. Chem. C*, 2020, **8**, 1811–1818.
- 43 A. Khanina, A. Novitskii, D. Pashkova, A. Voronin, T. Mori and V. Khovaylo, *Phys. Chem. Chem. Phys.*, 2024, **26**, 13006–13011.
- 44 L.-D. Zhao, J. He, D. Berardan, Y. Lin, J.-F. Li, C.-W. Nan and N. Dragoe, *Energy Environ. Sci.*, 2014, **7**, 2900–2924.
- 45 F. Li, J.-F. Li, L.-D. Zhao, K. Xiang, Y. Liu, B.-P. Zhang, Y.-H. Lin, C.-W. Nan and H.-M. Zhu, *Energy Environ. Sci.*, 2012, **5**, 7188–7195.
- 46 J. Sui, J. Li, J. He, Y.-L. Pei, D. Berardan, H. Wu, N. Dragoe, W. Cai and L.-D. Zhao, *Energy Environ. Sci.*, 2013, **6**, 2916–2920.
- 47 T. Kanno, H. Tamaki, H. K. Sato, S. D. Kang, S. Ohno, K. Imasato, J. J. Kuo, G. J. Snyder and Y. Miyazaki, *Appl. Phys. Lett.*, 2018, **112**, 033903.
- 48 I. Serhiienko, A. Novitskii, F. Garmroudi, E. Kolesnikov, E. Chernyshova, T. Sviridova, A. Bogach, A. Voronin, H. D. Nguyen, N. Kawamoto *et al.*, *Adv. Sci.*, 2024, 2309291.
- 49 L. Zhao, D. Berardan, Y. Pei, C. Byl, L. Pinsard-Gaudart and N. Dragoe, *Appl. Phys. Lett.*, 2010, **97**, 092118.
- 50 J. Li, J. Sui, Y. Pei, C. Barreteau, D. Berardan, N. Dragoe, W. Cai, J. He and L.-D. Zhao, *Energy Environ. Sci.*, 2012, **5**, 8543–8547.
- 51 J.-L. Lan, Y.-C. Liu, B. Zhan, Y.-H. Lin, B. Zhang, X. Yuan, W. Zhang, W. Xu and C.-W. Nan, *Adv. Mater.*, 2013, **25**, 5086–5090.
- 52 M. Zhang, J. Yang, Q. Jiang, L. Fu, Y. Xiao, Y. Luo, D. Zhang, Y. Cheng and Z. Zhou, *J. Electron. Mater.*, 2015, **44**, 2849–2855.
- 53 Y. Liu, J. Ding, B. Xu, J. Lan, Y. Zheng, B. Zhan, B. Zhang, Y. Lin and C. Nan, *Appl. Phys. Lett.*, 2015, **106**, 233903.
- 54 G.-K. Ren, S. Butt, K. J. Ventura, Y.-H. Lin, C.-W. Nan *et al.*, *RSC Adv.*, 2015, **5**, 69878–69885.
- 55 Y. Liu, L.-D. Zhao, Y. Zhu, Y. Liu, F. Li, M. Yu, D.-B. Liu, W. Xu, Y.-H. Lin and C.-W. Nan, *Adv. Energy Mater.*, 2016, **6**, 1502423.
- 56 D. Yang, X. Su, Y. Yan, T. Hu, H. Xie, J. He, C. Uher, M. G. Kanatzidis and X. Tang, *Chem. Mat.*, 2016, **28**, 4628–4640.
- 57 T.-L. Chou, G. C. Tewari, D. Srivastava, A. Yamamoto, T.-S. Chan, Y.-Y. Hsu, J.-M. Chen, H. Yamauchi and M. Karppinen, *Mater. Chem. Phys.*, 2016, **177**, 73–78.
- 58 B. Feng, G. Li, Z. Pan, Y. Hou, C. Zhang, C. Jiang, J. Hu, Q. Xiang, Y. Li, Z. He *et al.*, *Mater. Lett.*, 2018, **217**, 189–193.
- 59 B. Feng, G. Li, X. Hu, P. Liu, R. Li, Y. Zhang, Y. Li, Z. He and X. Fan, *J. Electron. Mater.*, 2020, **49**, 611–620.
- 60 B. Feng, X. Jiang, Z. Pan, L. Hu, X. Hu, P. Liu, Y. Ren, G. Li, Y. Li *et al.*, *Mater. Des.*, 2020, **185**, 108263.
- 61 H. Kang, X. Zhang, Y. Wang, J. Li, D. Liu, Z. Chen, E. Guo, X. Jiang and T. Wang, *Mater. Res. Bull.*, 2020, **126**, 110841.
- 62 T. He, X. Li, J. Tang, X. Zuo, Y. Zheng, D. Zhang, G. Tang *et al.*, *J. Alloys Compd.*, 2020, **831**, 154755.
- 63 Y. Katsura, M. Kumagai, T. Kodani, M. Kaneshige, Y. Ando, S. Gunji, Y. Imai, H. Ouchi, K. Tobita, K. Kimura *et al.*, *Sci. Technol. Adv. Mater.*, 2019, **20**, 511–520.

— Supplementary Information —

Pisarenko's Formula for the Thermopower

Andrei Novitskii^a and Takao Mori^{*a,b}

^a*Research Center for Materials Nanoarchitectonics (MANA),
National Institute for Materials Science (NIMS),
1-1 Namiki, Tsukuba, Ibaraki, 305-0044, Japan.*

^b*Graduate School of Pure and Applied Sciences,
University of Tsukuba,
1-1-1 Tennodai, Tsukuba, Ibaraki, 305-8573, Japan.*

*E-mail: MORI.Takao@nims.go.jp

Effective Mass Model

The outline of this section generally follows the books of V.I. Firsul' and P.S. Kireev with additional contributions taken from the book of B.M. Askerov.^{1,2,3} In solids, electron transport can be described in the Boltzmann transport theory framework. The effective mass model can be applied to materials with carrier transport dominated by majority carriers with a single scattering mechanism. In this case, the energy dependence of the relaxation time τ depends on the scattering mechanism and is expressed by a simple power-law

$$\tau(\varepsilon) = \tau_0 \varepsilon^r. \quad (\text{S1})$$

Here, τ_0 is a reference relaxation time for carriers at $k_B T$, $\varepsilon = E/k_B T$ represents the reduced carrier energy, and r represents the scattering factor ($r = -1/2$ for acoustic phonon scattering, $r = 1/2$ for polar optical phonon scattering, $r = 3/2$ for ionized-impurity scattering, etc.). By using the expression for density of states

$$g(E) = \frac{1}{2\pi^2} \left(\frac{2m_d^*}{\hbar^2} \right)^{3/2} \sqrt{E}, \quad (\text{S2})$$

the Fermi-Dirac distribution function

$$f(E, \mu) = \frac{1}{1 + e^{(E - \mu)/k_B T}}, \quad E = \frac{\hbar^2 k_B^2}{2m_d^*} \text{ (for single parabolic band)}, \quad (\text{S3})$$

the charge carrier concentration can be obtained through

$$n = \int_0^\infty g(E) f(E) dE = 4\pi \left(\frac{2m_d^* k_B T}{\hbar^2} \right)^{3/2} F_{1/2}(\eta). \quad (\text{S4})$$

Here m_d^* is the density of states effective mass $m_d^* = N_v^{2/3} \sqrt[3]{m_x^* m_y^* m_z^*}$ (N_v is the valley degeneracy factor), \hbar is the Planck constant, E is the charge carrier energy measured from the conduction band bottom E_c (or valence band maxima E_v), μ representing the free energy per electron, and $F_{1/2}(\eta)$ is the Fermi integral of order 1/2. The j -th order Fermi integrals are defined as

$$F_j(\eta) = \int_0^\infty \frac{\varepsilon^j}{1 + e^{\varepsilon - \eta}} d\varepsilon, \quad (\text{S5})$$

with $\eta = \mu/k_B T$ representing reduced Fermi energy and also known as reduced chemical potential.

In the Boltzmann transport theory framework with relaxation time approximation, the thermopower is expressed by¹

$$\alpha = \pm \frac{k_B}{e} \left[\frac{\int_0^\infty \varepsilon^{5/2} \tau(\varepsilon) \frac{\partial f(\varepsilon)}{\partial \varepsilon} d\varepsilon}{\int_0^\infty \varepsilon^{3/2} \tau(\varepsilon) \frac{\partial f(\varepsilon)}{\partial \varepsilon} d\varepsilon} - \eta \right]. \quad (\text{S6})$$

Considering Eqs. S1, S3, and S5, Eq. S6 can be rewritten as

$$\alpha(\eta) = \pm \frac{k_B}{e} \left(\frac{(r + 5/2) F_{r+3/2}(\eta)}{(r + 3/2) F_{r+1/2}(\eta)} - \eta \right). \quad (\text{S7})$$

Note that this formula is obtained by completely ignoring the temperature dependence of chemical potential, i.e. assuming $\eta \approx E_F/k_B T$, which can be non-negligible in some cases.⁴ The electrical conductivity, in turn, is expressed as¹

$$\sigma = \frac{8\pi e^2 (2m_d^* k_B T)^{3/2}}{3m_d^* \hbar^3} \int_0^\infty \varepsilon^{3/2} \tau(\varepsilon) \frac{\partial f(\varepsilon)}{\partial \varepsilon} d\varepsilon, \quad (\text{S8})$$

and can be simplified to

$$\sigma(\eta) = \frac{8\pi e (2m_d^* k_B T)^{3/2}}{3\hbar^3} \mu_0 \left(r + \frac{3}{2} \right) F_{r+1/2}(\eta) \quad (\text{S9})$$

with e representing the electron charge and μ_0 representing the intrinsic carrier mobility. Instead of μ_0 and m_d^* it is more convenient to express $\sigma(\eta)$ via the weighted mobility $\mu_w = \mu_0 (m_d^*/m_e)^{3/2}$:

$$\sigma(\eta) = \frac{8\pi e (2m_e k_B T)^{3/2}}{3\hbar^3} \mu_w \left(r + \frac{3}{2} \right) F_{r+1/2}(\eta). \quad (\text{S10})$$

The weighted mobility μ_w , in turn, is easy to calculate from experimentally measured thermopower α and electrical conductivity σ .⁵ It can also be considered as a descriptor for thermoelectric performance implemented in the so-called quality factor $\beta \propto \mu_w/\kappa_{lat}$ (κ_{lat} is the lattice (phonon) thermal conductivity).^{6,7,8}

Other transport coefficients, such as Lorenz number L and Hall factor r_H are expressed as functions of only η :^{1,3}

$$L(\eta) = \left(\frac{k_B}{e}\right)^2 \left(\frac{(r+7/2) F_{r+5/2}(\eta)}{(r+3/2) F_{r+1/2}(\eta)} - \left[\frac{(r+5/2) F_{r+3/2}(\eta)}{(r+3/2) F_{r+1/2}(\eta)} \right]^2 \right), \quad (S11)$$

$$r_H = \frac{3}{2} F_{1/2}(\eta) \frac{(2r+3/2) F_{2r+1/2}(\eta)}{(r+3/2)^2 F_{r+1/2}^2(\eta)}. \quad (S12)$$

Different $F_j(\eta)$ can be solved numerically for different values of η . However, for the two distinct regions of the chemical potential values, referred to as non-degenerate and degenerate limit, the Fermi integrals can be solved analytically, providing relatively simple expressions for the transport coefficients.

In the degenerate limit ($\eta \geq 5$) $F_j(\eta)$ can be expressed into a power series^{1,2}

$$F_j(\eta) = \frac{\eta^{j+1}}{j+1} + \frac{j\pi^2}{6} \eta^{j-1} + \dots \quad (S13)$$

The transport coefficients are then

$$n(\eta) = \frac{8\pi}{3} \left(\frac{2m_d^* k_B T}{h^2} \right)^{3/2} \eta^{3/2}, \quad (S14)$$

$$\sigma(\eta) = \frac{8\pi e (2m_e k_B T)^{3/2}}{3h^3} \mu_w \eta^{r+3/2}, \quad (S15)$$

$$L = \left(\frac{k_B}{e}\right)^2 \frac{\pi^2}{3}, \quad (S16)$$

$$r_H = 1, \quad (S17)$$

and

$$\alpha(\eta) = \pm \frac{k_B}{e} \frac{\pi^2}{3} \frac{r+3/2}{\eta}. \quad (S18)$$

By combining Eqs. S14 and S18, one obtains the well-known formula for the thermopower in degenerate semiconductors³

$$\alpha = \frac{8\pi^2 k_B^2 T}{3eh^2} m_d^* \left(\frac{\pi}{3n} \right)^{2/3} \left(r + \frac{3}{2} \right). \quad (S19)$$

In the non-degenerate limit ($\eta \leq -1$) where Fermi-Dirac statistics can be replaced with Boltzmann statistics, $F_j(\eta)$ can be approximated with a Maxwellian distribution^{3,1}

$$F_j(\eta) = \Gamma(j+1) e^\eta, \quad (S20)$$

where

$$\Gamma(j) = \int_0^\infty x^{j-1} e^{-x} dx, \quad (S21)$$

is the first-order Euler integral or the gamma function. The transport coefficients are then

$$n(\eta) = 2 \left(\frac{2\pi m_d^* k_B T}{h^2} \right)^{3/2} e^\eta, \quad (S22)$$

$$\sigma(\eta) = \frac{8\pi e (2m_e k_B T)^{3/2}}{3h^3} \mu_w \left(r + \frac{3}{2} \right) \Gamma\left(r + \frac{3}{2} \right) e^\eta, \quad (S23)$$

$$L = \left(\frac{k_B}{e}\right)^2 \left(r + \frac{5}{2} \right), \quad (S24)$$

$$r_H = \Gamma\left(\frac{5}{2} \right) \frac{\Gamma(2r+5/2)}{(\Gamma(r+5/2))^2}, \quad (S25)$$

and

$$\alpha(\eta) = \pm \frac{k_B}{e} \left(r + \frac{5}{2} - \eta \right). \quad (\text{S26})$$

By combining Eqs. S22 and S26, one obtains the Pisarenko formula for the thermopower in non-degenerate semiconductors⁷

$$\alpha = \pm \frac{k_B}{e} \left(r + \frac{5}{2} + \ln \frac{2(2\pi m_d^* k_B T)^{3/2}}{h^3 n} \right). \quad (\text{S27})$$

The comparison between the $F_{1/2}(\eta)$, $n(\eta)$, $L(\eta)$, $r_H(\eta)$, and $\alpha(\eta)$ calculated by using numerical solution for the case of deformation potential scattering (acoustic phonon scattering; $r = -1/2$) and by considering non-degenerate and degenerate limits is shown in Figure S1.

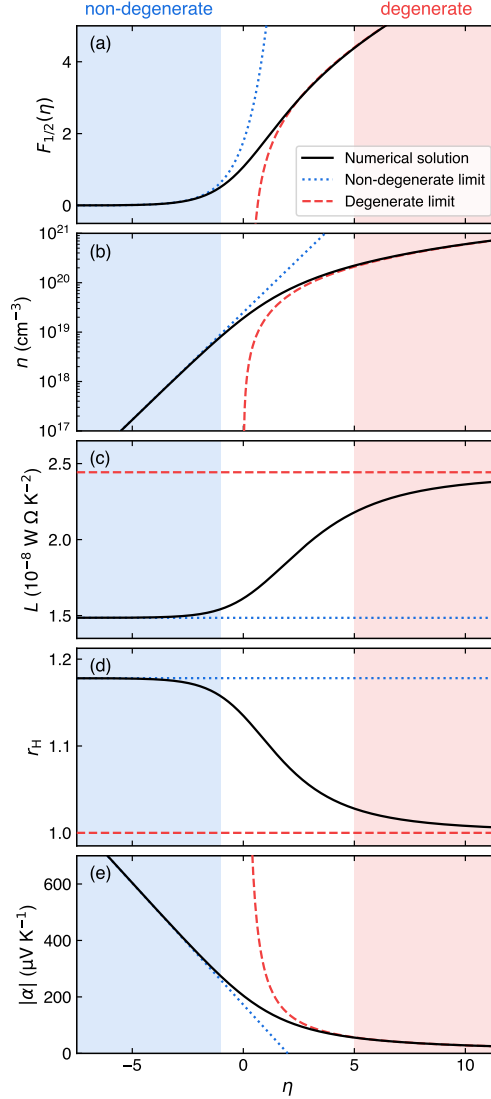


Figure S1: (a) Fermi integral $F_{1/2}$, (b) carrier concentration n , (c) Lorenz number L , (d) Hall factor r_H , and (e) thermopower α calculated in the two limits, namely degenerate (dashed lines) and non-degenerate (dotted lines), compared to the numerical solution (solid lines). The calculation was carried out assuming acoustic phonon scattering ($r = -1/2$).

Effective Mass in Case of Different Scattering Mechanisms

The reliability of the effective mass m_d^* estimation using the Pisarenko formula (Eq. S27) should also depend on the scattering mechanism (r value) and the value of the thermopower α (chemical potential η) as shown in Figure S2. From Figure S2 it is evident that m_d^* can be estimated via Pisarenko formula (Eq. S27) for materials with $|\alpha|$ higher than $130 - 150 \mu\text{V K}^{-1}$.

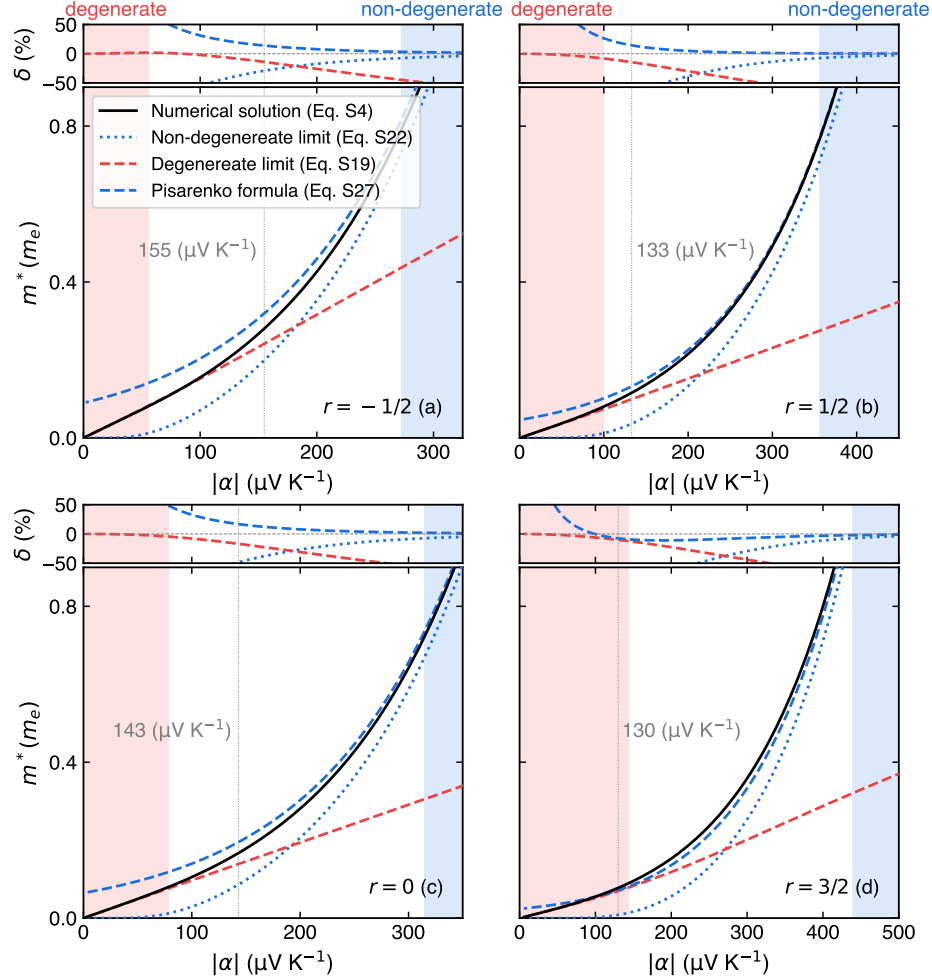


Figure S2: Effective mass m_d^* as a function of the thermopower α , calculated using the full numerical solution (Eq. S4, black solid curve), the non-degenerate limit (Eq. S22, dotted curve), the degenerate limit (Eq. S19, red dashed curve), and Pisarenko formula (Eq. S27, blue dashed curve) for different scattering mechanisms: (a) acoustic phonon scattering, (b) polar optical scattering, (c) neutral impurity scattering, and (d) ionized impurity scattering. Calculations assume a constant charge carrier concentration $n = 5 \cdot 10^{18} \text{ cm}^{-3}$. The upper panels in each subplot show the relative difference δ in m_d^* values obtained using the corresponding formulas. The thin gray dotted lines indicate the α value at which the δ between m_d^* calculated using Eq. S19 and Eq. S27 is equal and represent the boundary of applicability for these formulas.

Thermopower in Case of Different Scattering Mechanisms

Change in the chemical potential η is equivalent to the carrier concentration n adjustment by doping (see Eq. S4), thus the α vs. n (log-scale) plot (known as the Pisarenko plot) is essentially confirming the same range of the Pisarenko formula applicability as discussed in the main text (Figure S3).

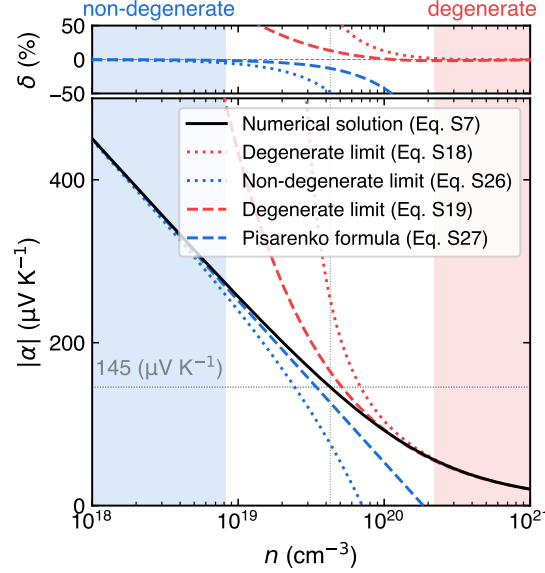


Figure S3: Pisarenko plot (α vs. n in a log-scale) with $\alpha(n)$ calculated through full numerical solution (Eq. S7, black solid curve), the degenerate limit (Eq. S18, red dotted curve), the non-degenerate limit (Eq. S26, blue dotted curve), and two analytical formulas for degenerate (Eq. S19, red dashed curve) and non-degenerate (Pisarenko formula, Eq. S27, blue dashed curve) semiconductors. The calculations assume acoustic phonon scattering with $r = -1/2$ and $m_d^* = m_e$. The upper panel shows δ , the relative difference in α calculated using the corresponding formulas. The thin gray dotted lines indicate the threshold where δ between α values calculated from Eq. S19 and Eq. S27 is equal and reaches $\approx 13\%$, representing the limits of their applicability.

In the case of polar optical scattering at relatively high temperatures ($E > h\nu$, where E is the electron energy and ν is the maximum frequency of longitudinal lattice vibrations) $r = 1/2$.⁹ As shown in Figure S4, in case of $r = 1/2$ the Pisarenko formula can be used up to $\eta \approx 3.6$ ($|\alpha| \approx 127 \mu\text{V K}^{-1}$). In low temperature region ($E < h\nu$) where $r = 0$,⁹ the Pisarenko formula is applicable up to $\eta \approx 2.4$ ($|\alpha| \approx 133 \mu\text{V K}^{-1}$).

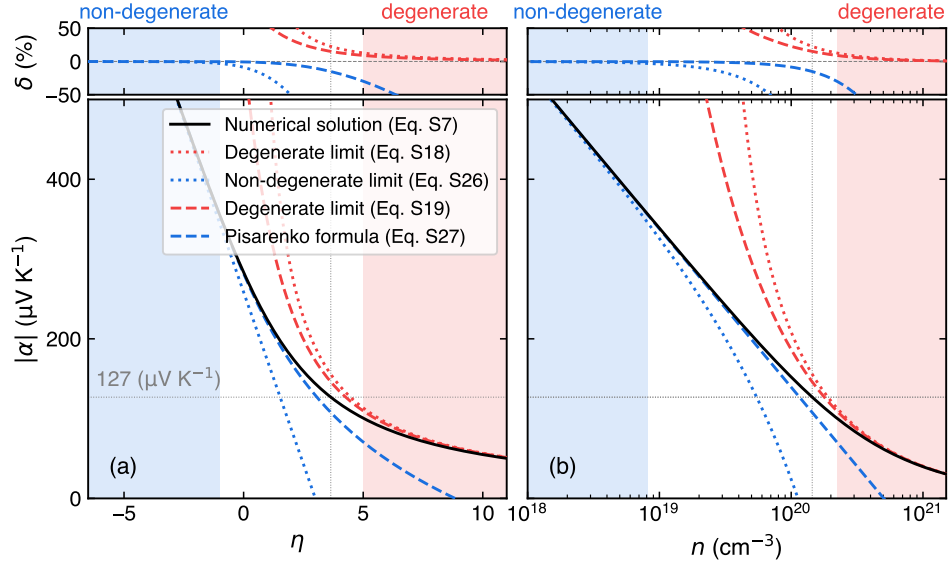


Figure S4: Thermopower α as a function of (a) chemical potential η and (b) carrier concentration n calculated through numerical solution (Eq. S7, black solid curve), the degenerate limit (Eq. S18, red dotted curve), the non-degenerate limit (Eq. S26, blue dotted curve), and two analytical formulas for degenerate (Eq. S19, red dashed curve) and non-degenerate (Pisarenko formula, Eq. S27, blue dashed curve) semiconductors. The calculations assume polar optical phonon scattering ($r = 1/2$) and $m_d^* = m_e$. The upper panel shows δ , the relative difference in α calculated using the corresponding formulas. The thin gray dotted lines indicate the threshold where δ between α values calculated from Eq. S19 and Eq. S27 is equal and reaches $\approx 15\%$, representing the limits of their applicability.

In the case of ionized impurity scattering ($r = 3/2$), the Pisarenko formula formally agrees well with the full numerical solution up to $\eta \approx 8.9$ ($|\alpha| \approx 90 \mu\text{V K}^{-1}$) as shown in Figure S5. However, it can be noted that for $\eta > 6$, both the Pisarenko formula (Eq. S27) and the formula for degenerate semiconductors (Eq. S19) show good agreement with the thermopower values calculated by Eq. S7 within 10 % accuracy. In this case, it might be reasonable to use the formula for degenerate semiconductors for $\eta > 6$, while in the intermediate degeneracy range (from $\eta = -1$ to $\eta = 6$) the Pisarenko formula can be used to estimate the thermopower as a function of η (or n).

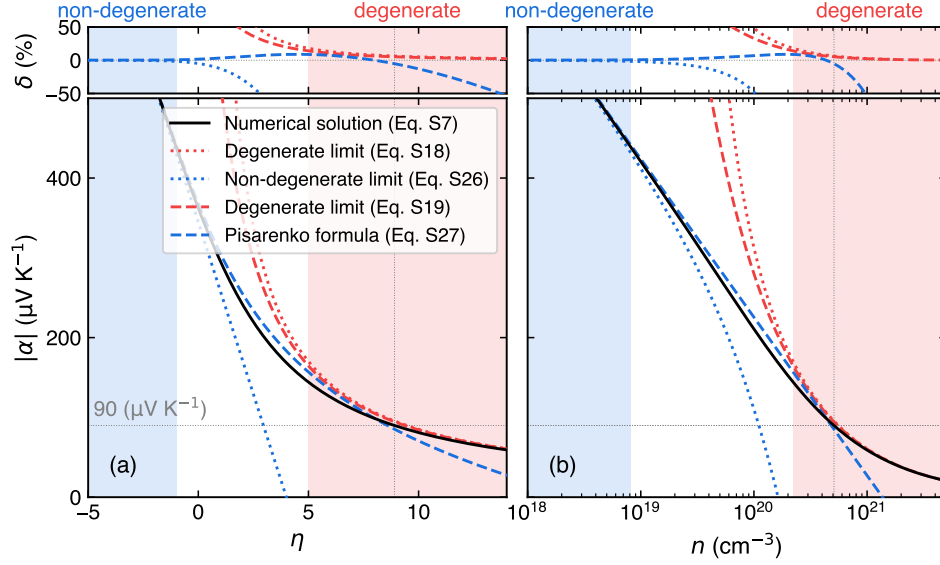


Figure S5: Thermopower α as a function of (a) chemical potential η and (b) carrier concentration n calculated through numerical solution (Eq. S7, black solid curve), the degenerate limit (Eq. S18, red dotted curve), the non-degenerate limit (Eq. S26, blue dotted curve), and two analytical formulas for degenerate (Eq. S19, red dashed curve) and non-degenerate (Pisarenko formula, Eq. S27, blue dashed curve) semiconductors. The calculations assume ionized impurity scattering ($r = 3/2$) and $m_d^* = m_e$. The upper panel shows δ , the relative difference in α calculated using the corresponding formulas. The thin gray dotted lines indicate the threshold where δ between α values calculated from Eq. S19 and Eq. S27 is equal and reaches $\approx 5\%$, representing the limits of their applicability.

The Thermopower-Conductivity Relations

For both degenerate and non-degenerate regions the thermopower-conductivity relations can be derived. The combination of Eqs. S15 and S18 yields the thermopower-conductivity relation in the degenerate limit ($|\alpha| \leq 56 \mu\text{V K}^{-1}$):

$$\alpha = \pm \frac{k_B}{e} \frac{\pi^2}{3} \left(r + \frac{3}{2} \right) \left(\frac{8\pi e (2m_e k_B T)^{3/2}}{3\sigma h^3} \mu_w \right)^{\frac{1}{r+3/2}}. \quad (\text{S28})$$

For non-degenerate limit ($|\alpha| \geq 273 \mu\text{V K}^{-1}$) the thermopower-conductivity relation can be obtained from the combination of Eqs. S23 and S26 or simply derived from Pisarenko formula shown in Eq. S27 by considering $\sigma = en\mu$:

$$\alpha = \pm \frac{k_B}{e} \left[\frac{5}{2} + r + \ln \left(\frac{8\pi e (2m_e k_B T)^{3/2}}{3h^3} \mu_w \Gamma \left(r + \frac{5}{2} \right) \right) - \ln \sigma \right]. \quad (\text{S29})$$

One can note that Pisarenko formula provides a good agreement with numerical solution down to $|\alpha| \approx 90 \mu\text{V K}^{-1}$ with less than 10 % error when plotted as α versus σ in a log-scale (Figure S6).

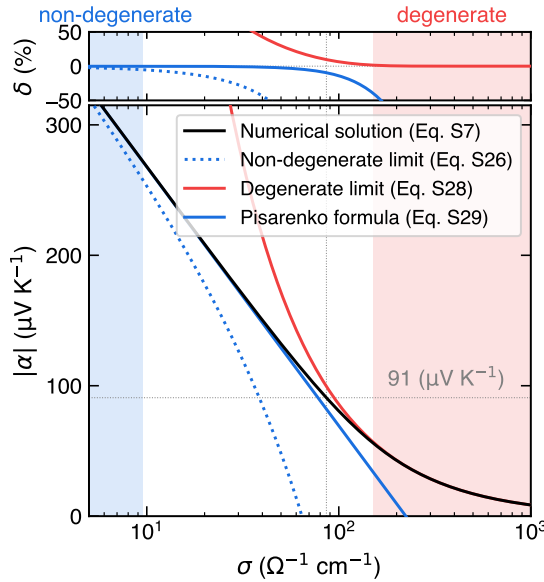


Figure S6: Jonker plot (α vs. σ in a log-scale) showing the thermopower-conductivity relation calculated using Eq. S10 for conductivity σ and the full numerical solution (Eq. S7, black solid curve), the non-degenerate limit (Eq. S26, dotted curve), the degenerate limit (Eq. S28, red solid curve), and the Pisarenko formula (Eq. S29, blue solid curve) for thermopower α . Calculations were performed assuming acoustic phonon scattering ($r = -1/2$) and a weighted mobility $\mu_w = 10 \text{ cm}^2 \text{ V}^{-1} \text{ s}^{-1}$. The upper panel shows δ , the relative difference in α calculated using the corresponding formulas. The thin gray dotted lines indicate the threshold where δ between α values calculated from Eq. S28 and Eq. S29 is equal and reaches $\approx 10\%$, representing the limits of their applicability.

When polar optical scattering is the main scattering mechanism of the charge carriers, the α vs. σ relation can be accurately (with less than 10 % error) described by the Pisarenko formula only up to $|\alpha| \approx 168 \mu\text{V K}^{-1}$, yet this extends significantly beyond the non-degenerate limit (Figure S7a). In the case of ionized impurity scattering, however, the Pisarenko formula accurately describes the α vs. σ relation only for $|\alpha| \geq 236 \mu\text{V K}^{-1}$ (Figure S7b).

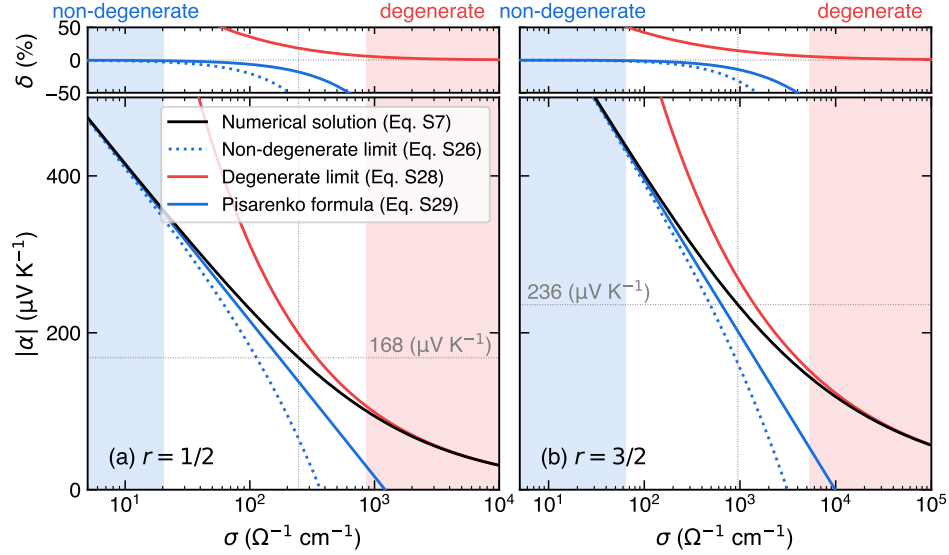


Figure S7: Jonker plot (α vs. σ in a log-scale) showing the thermopower-conductivity relation calculated using Eq. S10 for conductivity σ and the full numerical solution (Eq. S7, black solid curve), the non-degenerate limit (Eq. S26, dotted curve), the degenerate limit (Eq. S28, red solid curve), and the Pisarenko formula (Eq. S29, blue solid curve) for thermopower α . Calculations were performed assuming (a) polar optical phonon scattering ($r = 1/2$) and (b) ionized impurity scattering ($r = 3/2$). In both cases, the weighted mobility is $\mu_w = 10 \text{ cm}^2 \text{ V}^{-1} \text{ s}^{-1}$. The upper panel shows δ , the relative difference in α calculated using the corresponding formulas. The thin gray dotted lines indicate the threshold where δ between α values calculated from Eq. S28 and Eq. S29 is equal (approximately 17 % when $r = 1/2$ and 14 % when $r = 3/2$), representing the limits of their applicability.

Example of Jonker-type Analysis

Below is an example of how Jonker-type analysis at elevated temperatures can be utilized through the fitting of thermopower and power factor using the Pisarenko formula (Eqs. 13 and 15 in the main text). For materials where the weighted mobility does not significantly change with doping and temperature, it is possible to reveal the mechanism behind the power factor variation even without Hall data. In this case, the increase in charge carrier (hole) concentration is due to La substitution with Ba, as demonstrated in Figure S8.

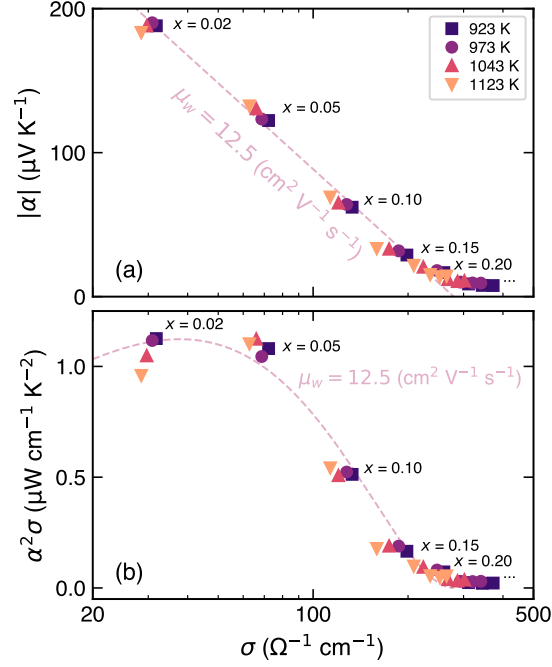


Figure S8: (a) Thermopower α and (b) power factor $\alpha^2 \sigma$ as functions of electrical conductivity σ for $\text{La}_{2-x}\text{Ba}_x\text{CuO}_4$ ($x = 0.02, 0.05, 0.10, 0.15, 0.20, 0.25, 0.30, 0.35$) at temperatures from 923 to 1123 K. Experimental data are taken from Ref. 10. The weighted mobility $\mu_w = 12.5 \text{ cm}^2 \text{ V}^{-1} \text{ s}^{-1}$ was obtained by fitting the experimental data with Eqs. 13 and 15, presented in the main text.

Temperature Dependence of the Thermopower

As discussed in the main text, the Pisarenko formula reasonably well describes the temperature dependence of the thermopower (Figure S9a), as well as the $\alpha(\sigma)$ (Figure S9b) and $\alpha^2\sigma(\sigma)$ (Figure S9c) relationships in lightly doped (partially degenerate) BiCuSeO oxyselenides. Deviations from the curves predicted by the Pisarenko formula are attributed to (1) a mixed scattering mechanism at low temperatures (gray area in Figure S9) and (2) bipolar conduction at high temperatures (light gray area in Figure S9).

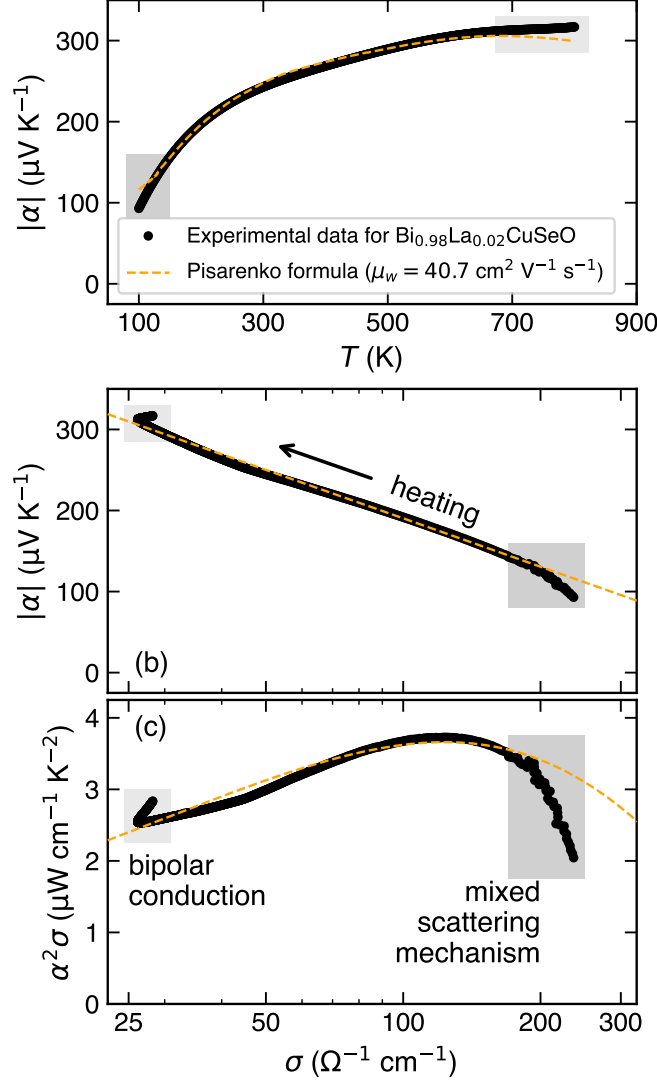


Figure S9: (a) Temperature-dependent thermopower α , (b) thermopower α , and (c) power factor $\alpha^2\sigma$ as functions of electrical conductivity σ for Bi_{0.98}La_{0.02}CuSeO (data from Ref. 11). The experimental data were fitted by the Pisarenko formula (Eq. S29), yielding a weighted mobility $\mu_w = 40.7 \text{ cm}^2 \text{ V}^{-1} \text{ s}^{-1}$.

References

- [1] Fistul', V. I. *Heavily Doped Semiconductors*; Springer: New York, 1969.
- [2] Kireev, P. S. *Semiconductor Physics*; Mir Publishers: Moscow, 1978.
- [3] Askerov, B. M. *Electron Transport Phenomena in Semiconductors*; World Scientific: Singapore, 1994.
- [4] Takeuchi, T.; Toyama, Y.; Yamamoto, A. Role of Temperature Dependent Chemical Potential on Thermoelectric Power. *Mater. Trans.* **2010**, *51*, 421–427.
- [5] Snyder, G. J.; Snyder, A. H.; Wood, M.; Gurunathan, R.; Snyder, B. H.; Niu, C. Weighted Mobility. *Adv. Mater.* **2020**, *32*, 2001537.
- [6] Chasmar, R.; Stratton, R. The Thermoelectric Figure of Merit and Its Relation to Thermoelectric Generators. *Int. J. Electron.* **1959**, *7*, 52–72.
- [7] Ioffe, A. F. *Semiconductor Thermoelements, and Thermoelectric Cooling*; Infosearch: London, 1957.
- [8] Yan, J.; Gorai, P.; Ortiz, B.; Miller, S.; Barnett, S. A.; Mason, T.; Stevanović, V.; Toberer, E. S. Material Descriptors for Predicting Thermoelectric Performance. *Energy & Environmental Science* **2015**, *8*, 983–994.
- [9] Davydov, B. J.; Shmushkevich, I. M. Theory of Electronic Semiconductors. I (In Russian). *Usp. Fiz. Nauk* **1940**, *24*, 21–67.
- [10] Su, M.-Y.; Elsbernd, C. E.; Mason, T. O. Jonker “Pecir” Analysis of Oxide Superconductors. *J. Am. Ceram. Soc.* **1990**, *73*, 415–419.
- [11] Novitskii, A.; Serhiienko, I.; Novikov, S.; Ashim, Y.; Zheleznyi, M.; Kuskov, K.; Pankratova, D.; Konstantinov, P.; Voronin, A.; Tretiakov, O. A.; Inerbaev, T.; Burkov, A.; Khovaylo, V. Influence of Bi Substitution with Rare-Earth Elements on the Transport Properties of BiCuSeO Oxyselenides. *ACS Appl. Energy Mater.* **2022**, *5*, 7830–7841.